J. Iron Steel Res. Int.
https://doi.org/10.1007/s42243-018-0093-4

ORIGINAL PAPER

Controllable SiO_2 coating layer of FeSiBPNb amorphous powder cores with excellent soft magnetic properties

Ke-yu Huang[1,2] · Ya-qiang Dong[2] · Min Liu[2] · Ji-hang Ren[1] · Shu-han Lu[1] · Zhan-kui Zhao[1] · Chun-tao Chang[2] · Xin-min Wang[2]

Received: 5 December 2017 / Revised: 16 March 2018 / Accepted: 22 March 2018

Abstract
Amorphous powder cores based on spherical $(Fe_{0.76}Si_{0.09}B_{0.1}P_{0.05})_{99}Nb_1$ amorphous powder and their SiO_2 layer prepared by in situ coating insulation process were investigated in detail. These cores were characterized by scanning electron microscopy and X-ray diffraction analyses, and the results revealed that the surface layer of the amorphous powder was composed of SiO_2 with uniform surface coverage. The thickness of the SiO_2 insulating layer could be controlled by adjusting the tetraethyl orthosilicate (TEOS) content. By cold-pressing with epoxy resin under a pressure of 1800 MPa, a ring powder core with an outer diameter of 20.3 mm, inner diameter of 12.7 mm, and height of 5.3 mm was prepared. The FeSiBPNb composite core showed its best properties when the TEOS content was 2 mL/g (the volume of TEOS for each gram of $(Fe_{0.76}Si_{0.09}B_{0.1}P_{0.05})_{99}Nb_1$ amorphous powder, mL/g), which showed good relative permeability in the high-frequency range of up to 10 MHz and a low core loss of 320 W/kg under the maximum magnetic flux density of 0.1 T and frequency of 100 kHz.

Keywords Soft magnetic composite · Core loss · Relative permeability · In situ chemical deposition · Amorphous powder

1 Introduction

Fe-based amorphous alloys have attracted widespread attention in the last two decades due to their excellent magnetic properties, which facilitate their application in the fabrication of soft magnetic powder cores with remarkable relative permeability (μ_r), high saturation magnetization (M_s), and low coercive force (H_c) [1–6]. These advantages help mitigate energy consumption and noise pollution, and hence, this class of alloys has wide potential for application to transformers, generators, and electrical equipment in the high-frequency range [7–11]. Recently, a new Fe-based bulk glassy magnetic alloy, $(Fe_{0.76}Si_{0.09}B_{0.1}P_{0.05})_{99}Nb_1$, which had a high M_s value, strong glass-forming ability (GFA), and excellent magnetic properties, was developed [12, 13]. Such high GFA may allow researchers to produce spherical glassy alloy powders by gas atomization [14]. Moreover, a uniform insulating coating layer can be easily created on the surface of spherical amorphous powder, which can reduce the core loss of soft magnetic cores.

Three components make up the core loss: eddy current loss (P_e), hysteresis loss (P_h), and residual loss (P_r). For high-frequency applications, it is necessary to decrease the core loss while improving the efficiency of energy conversion [15, 16]. At high frequencies, the eddy current loss is the major core loss component, which may be lowered if there is good electro-insulation between particles. Usually, organic or inorganic insulating materials are deposited on the surface of the powder prior to cold-pressing, so that a

✉ Ya-qiang Dong
dongyq@nimte.ac.cn

✉ Zhan-kui Zhao
zhaozk@ccut.edu.cn

✉ Chun-tao Chang
ctchang@nimte.ac.cn

[1] College of Materials Science and Engineering, Changchun University of Technology, Changchun 130012, Jilin, China

[2] Zhejiang Province Key Laboratory of Magnetic Materials and Application Technology, CAS Key Laboratory of Magnetic Materials and Devices, Ningbo Institute of Materials Technology and Engineering, Chinese Academy of Sciences, Ningbo 315201, Zhejiang, China

Published online: 14 June 2018

thin layer of an insulating material can be formed and the particles are electrically separated from one another [17–19].

The present work aims to obtain the optimal insulating effect. SiO_2, which has high electrical resistivity, was used as the insulating layer to prepare soft magnetic composites (SMCs) [20, 21]. However, as a kind of inorganic materials, SiO_2 is nonmagnetic and thus will reduce magnetic induction. Therefore, it is very important to achieve a balance between low core loss and high magnetic induction by controlling the amount of insulation material. Conventional high-energy ball milling is a convenient method in this regard, but it destroys the sphericity of the particles and introduces impurities from the milling balls [22, 23]. In order to solve this problem, in this work, SiO_2 was first coated on spherical $(Fe_{0.76}Si_{0.09}B_{0.1}P_{0.05})_{99}Nb_1$ amorphous powders through in situ chemical deposition. Then, SMCs were prepared by combining the FeSiBPNb@SiO_2 core–shell particles with epoxy resin to generate a double core–shell insulating layer, which is crucial to ensure that the eddy current loss in the amorphous powder cores (APCs) is relatively low. The thickness of the SiO_2 insulating layer was regulated in order to ensure the optimal conditions, and the magnetic properties were analyzed in detail.

2 Experimental

2.1 Synthesis of FeSiBPNb amorphous powders via gas atomization

The $(Fe_{0.76}Si_{0.09}B_{0.1}P_{0.05})_{99}Nb_1$ alloy ingot was produced by induction melting of a mixture of Fe, Si, B, Nb, and pre-alloy Fe_3P ingots in a pure argon atmosphere. The atomization method under a high-pressure gas atmosphere was applied to fabricate amorphous metallic powders. The ingot was melted again in a quartz tube by using a vacuum induction heating coil. The ingot was introduced into the quartz tube by means of a nozzle with 0.8 mm diameter and atomized by high-pressure argon with a dynamic pressure of 7 MPa.

2.2 Design of amorphous FeSiBPNb@SiO_2 composite particles

The FeSiBPNb amorphous powder sieved to a particle size of less than 75 μm was used for the following experiments. Tetraethyl orthosilicate (TEOS, 98 wt%), 3-triethoxysilypropylamine (APTES, 99 wt%), and aqueous ammonia (28 wt%, laboratory grade) were bought from Aladdin Industrial Corporation, China. All the chemicals were of analytical grade and used without further purification. In the coating process, 25 g of amorphous $(Fe_{0.76}Si_{0.09}B_{0.1}P_{0.05})_{99}Nb_1$ powder, 2 mL APTES, and 5 mL deionized water were stirred for 1 h at 50 °C and dispersed in 200 mL of absolute ethanol. Then, the reaction temperature was increased to 60 °C with 2 mL aqueous ammonia (25 wt%) and put into TEOS with contents of 1, 2, and 3 mL/g. After washing with absolute ethanol multiple times, the suspension was dried at 60 °C for 24 h.

2.3 Preparation of FeSiBPNb amorphous composite powder cores

The amorphous composite powder core was produced by using the FeSiBPNb@SiO_2 core–shell particles mentioned above. Ultrasonic cleaning in acetone solution was performed for 10 min to disperse the amorphous core–shell particles in the epoxy resin. The weight percentages of FeSiBPNb@SiO_2 and epoxy resin were 97 and 3%. Subsequently, stirring using glass rods was carried out until the acetone solution evaporated. The composite powder was dried at 70 °C for 30 min in an electrothermal constant-temperature drying furnace. Then, the coating of SiO_2 and epoxy resin on the amorphous powder was achieved.

The composite powder mixture was used to compact toroid cores with outer and inner diameters of 20.3 and 12.7 mm, respectively, at 1800 MPa. Then, the toroid cores were annealed at 400 °C for 1 h to reduce the internal stress caused by cold-pressing. For comparison, FeSiBPNb APCs with 1, 2, and 3 mL/g TEOS were produced under similar conditions.

2.4 Characterization

X-ray diffraction (XRD) analysis with Cu Kα radiation, as well as scanning electron microscopy (SEM) and differential scanning calorimetry (DSC), was carried out to probe the features of the gas-atomized powder. Impedance spectroscopy (HP 4244A) was used to measure the relative permeability spectrum from 10 kHz to 110 MHz. The DC bias field performance was evaluated using an Agilent 4980A system, and an AC *B–H* loop tracer was used to determine the losses of the soft magnetic powder core.

3 Results and discussion

Figure 1a, b presents the XRD patterns of the FeSiBPNb amorphous powders during in situ chemical deposition. Only the typical diffusion halo pattern due to the amorphous phase was observed, while no crystal phase peak was observed. This result shows that particles with sizes below 75 μm form a glassy phase without crystallinity. The XRD profile of the raw chemical SiO_2 deposit (Fig. 1c) showed

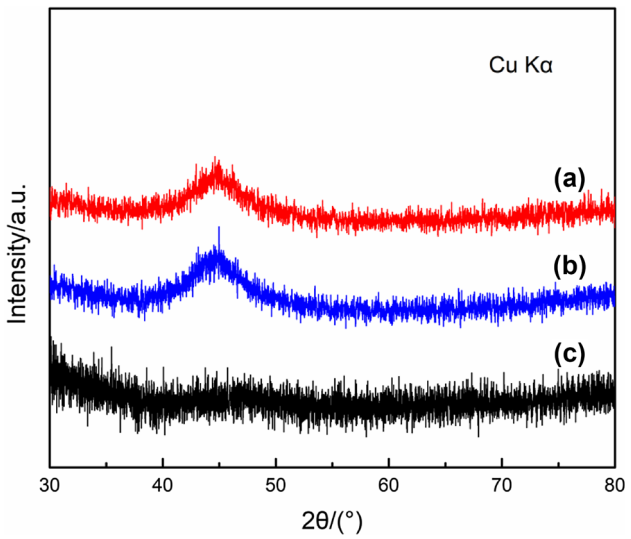

Fig. 1 XRD patterns of raw FeSiBPNb amorphous powder (a), in situ chemically deposited particles with a TEOS content of 2 mL/g (b), and raw chemical SiO_2 deposit (c)

an almost horizontal line, which indicated that the deposited SiO_2 was amorphous. Moreover, the deposits formed on the surface of the FeSiBPNb amorphous particles should be amorphous SiO_2 phases. All these results were consistent with the literature data [22].

The SEM image of the raw powder in Fig. 2a suggests that the amorphous FeSiBPNb-atomized powder is spherical. Uniform coating of the powder with the insulating material would help mitigate eddy current losses between the particles. The surface of the raw FeSiBPNb alloy particles was clear and flat, but became rougher after the in situ chemical deposition. Thus, the performance of the amorphous composite magnetic powder core will be greatly improved for use in the medium- and high-frequency applications. The FeSiBPNb@SiO_2@epoxy resin doubly insulated composite powders are presented in Fig. 2b. An epoxy resin coating layer is generated on the outer surface of the SiO_2 insulating layer. The epoxy resin also results in agglomeration of the particles, as seen in the SEM images. Figure 2c–e shows SEM images of the FeSiBPNb particles after in situ chemical deposition with TEOS contents of 1, 2, and 3 mL/g, respectively. Apparently, a uniform and thin insulating layer appears on the particle surface after in situ chemical deposition. Adjusting the TEOS content can help in regulating the thickness of the amorphous SiO_2 layer. As revealed by Fig. 2f–h, with an increase in the TEOS contents from 1 to 3 mL/g, the thickness of the SiO_2 layer increased from 148 to 305 nm. A distinct and high-quality insulating layer on the surface of the amorphous powders would be vital for fabricating SMCs with desired properties.

Figure 3 illustrates the frequency dependence of the μ_r of cores produced using different amounts of TEOS and 3 wt% epoxy resin. The μ_r strongly depends on the non-magnetic material content. It can be concluded from Fig. 3 that the μ_r of the cores decreases with further increase in the SiO_2 content, as the μ_r decreases from 53 to 44 when the TEOS content increases from 1 to 3 mL/g. The formation of a SiO_2 layer on the FeSiBPNb amorphous powders may reduce the μ_r, while the stability can be improved. All the cores with a steady μ_r to 10 MHz are well suited applicable for use in components for electronic systems, which require a consistent permeability at very high frequencies.

The core loss refers to the power absorbed by a core under the prescribed time-varying magnetic field. Further, the core loss is known to consist of P_h, P_e, and P_r [19]. The total loss (P_{cv}) can be expressed as follows:

$$P_{cv} = P_h + P_e + P_r \quad (1)$$

The P_r is significant only at very low induction levels and at very high frequencies, so it can be ignored in power applications. Thus, P_h and P_e account for most of the core loss. Figure 4 reflects the frequency dependence of the core loss. At 25–39 kHz, the P_{cv} increases with an increase in TEOS content, because high amounts of SiO_2 lead to a high P_h rate in the low-frequency range. On the other hand, the P_e is dominant in the high-frequency range, and it may be efficiently decreased through proper insulation of the magnet powder cores. Thus, the P_{cv} of the sample prepared with 1 mL/g of TEOS is larger than that of the 2 mL/g at 39 kHz; the core with 2 mL/g of TEOS shows the smallest loss among the three samples at frequencies above 39 kHz. The cores with 1 or 2 mL/g of TEOS show core losses of approximately 350 and 320 W/kg, respectively, at 100 kHz for B_m = 0.1 T. Furthermore, the cores produced using powders with 3 mL/g of TEOS exhibit the largest P_{cv} in the testing frequency range.

Figure 5 shows the μ_r percentage retained under a DC bias field at 100 kHz, which is defined as the ratio of permeabilities in the presence and absence of a DC bias field. These three cores retain over 70% of their μ_r under a field of 7962 A m^{-1}, indicating excellent DC bias performance. The well-distributed SiO_2 and epoxy resin on the amorphous powders can electrically separate the particles from one another, leading to high permeability retention. This result also implies that it is not so easy for the APCs to be saturated at a low applied magnetic field and might be applied to process the high output current in the power supply.

The magnetic properties of different powder core samples at 100 kHz are compared in Fig. 6. Although the DC bias of an FeSiB powder core is high, its μ_r is low at 100 kHz [24]. Compared to other powder cores [25–28],

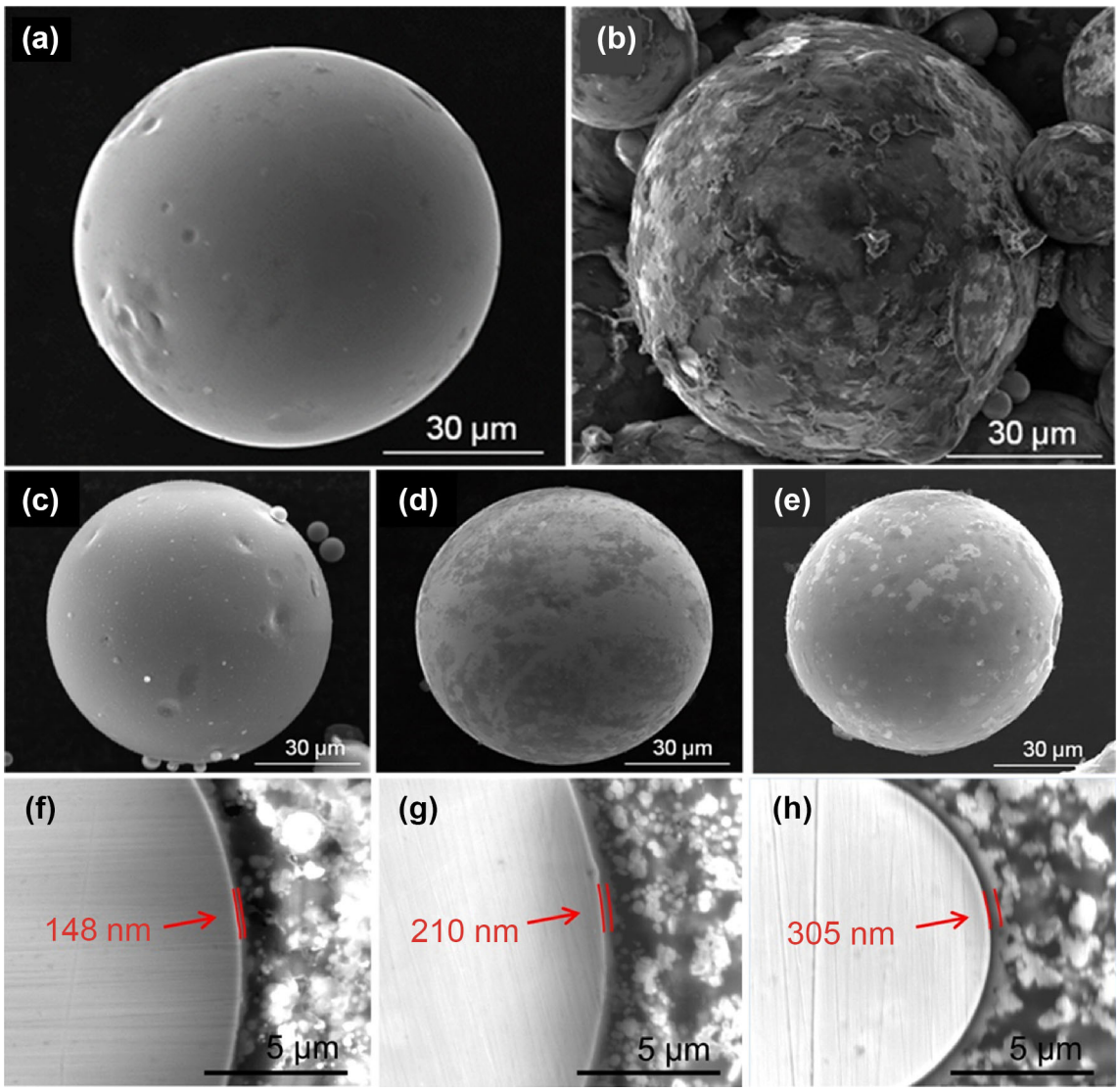

Fig. 2 SEM images of raw amorphous FeSiBPNb particles (**a**) and FeSiBPNb@SiO_2@epoxy resin doubly insulated composite powders (**b**), surface and cross-sectional images of FeSiBPNb@SiO_2 particles obtained via in situ chemical deposition with TEOS contents of 1 mL/g (**c**, **f**), 2 mL/g (**d**, **g**), and 3 mL/g (**e**, **h**)

the core in this work shows better DC bias performance in a similar μ_r range. In addition, an FeCuNbSiB powder core with a size of 250–850 μm has high μ_r but a low DC bias at 100 kHz [29]. In summary, the FeSiBPNb APCs coated with a SiO_2 layer shows superior performance in terms of μ_r and DC bias in the high-frequency range.

4 Conclusions

1. FeSiBPNb APCs shows low loss in various frequency ranges. When the core is applied in the high-frequency range, the chemical coating with 2 mL/g TEOS is optimal.
2. With decreasing TEOS content, the thickness of the SiO_2 layer decreases and the μ_r of the cores increases.
3. The magnetic cores exhibit excellent DC bias characteristics and maintain over 70% of the original μ_r at 7962 A m^{-1} outfield. The as-prepared intergranular insulated FeSiBPNb composite cores are expected to noticeably improve the energy conversion efficiency and reduce the energy consumption in electromagnetic switching devices.

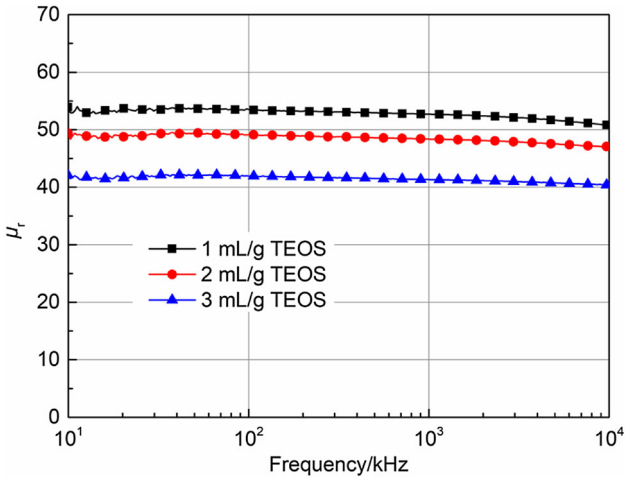

Fig. 3 Frequency dependence of μ_r of FeSiBPNb powder cores with various TEOS contents

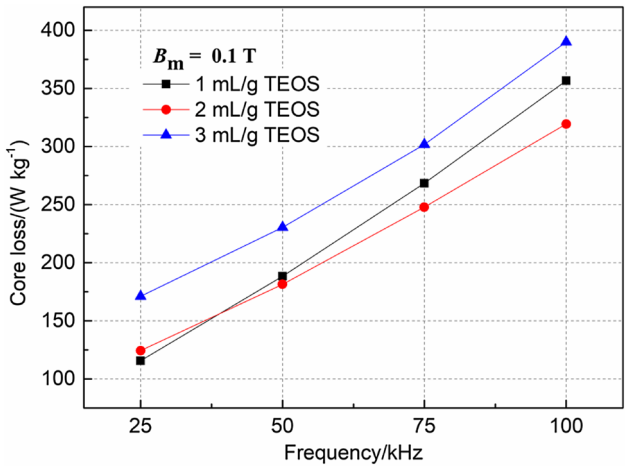

Fig. 4 Frequency dependence of core loss of FeSiBPNb powder cores with different TEOS contents and 3 wt% epoxy resin

Acknowledgements The work was with the support from the National Key Research and Development Program of China (Grant No. 2017YFB0903902), National Natural Science Foundation of China (Grant Nos. 51601205, 51671035, 51071034, and 51671206), and Ningbo Municipal Nature Science Foundation (Grant No. 2017A610036).

References

[1] E.A. Périgo, S. Nakahara, Y. Pittini-Yamada, Y. de Hazan, T. Graule, J. Magn. Magn. Mater. 323 (2011) 1938–1944.
[2] M. Yagi, I. Endo, I. Otsuka, H. Yamamoto, R. Okuno, H. Koshimoto, A. Shintani, J. Magn. Magn. Mater. 215 (2000) 284–287.
[3] A. Makino, K. Suzuki, A. Inoue, T. Masumoto, Mater. Trans. JIM 32 (1991) 551–556.
[4] B.V. Neamţu, T.F. Marinca, I. Chicinaş, O. Isnard, F. Popa, P. Păşcuţă, J. Alloy. Compd. 600 (2014) 1–7.
[5] S. Chen, Q. Zhao, Y. Qi, F. Liu, M. Wang, R. Jia, D. Zhu, M. Liu, X. Chen, A. Cheng, Poult Sci. 94 (2015) 17–24.

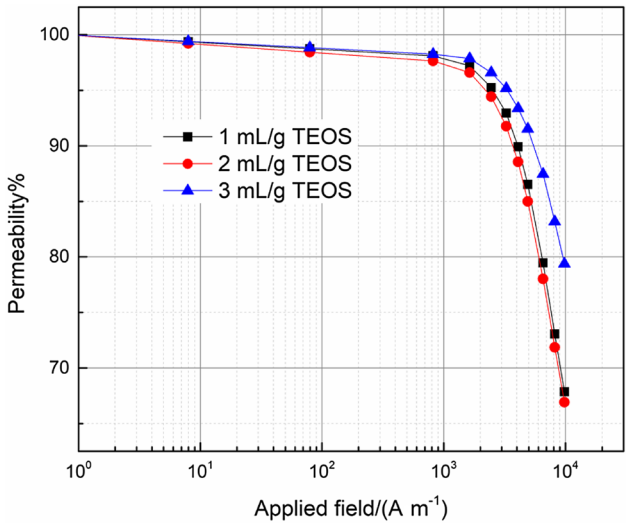

Fig. 5 Changes in μ_r retention ratio of FeSiBPNb powder cores with different TEOS contents under a DC bias field

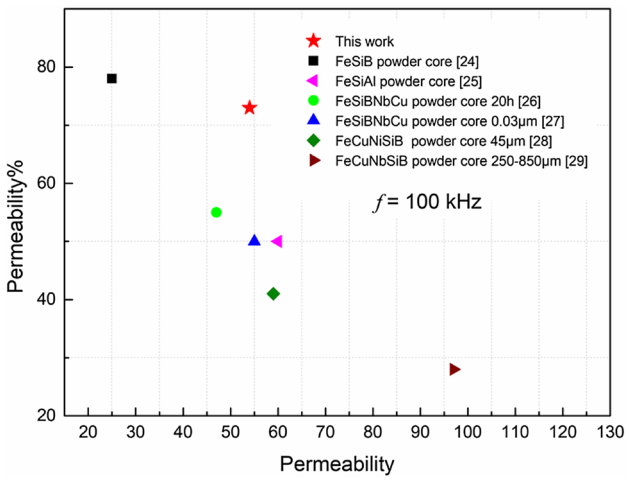

Fig. 6 μ_r and DC bias properties of different powder core samples at 100 kHz and under a field of 7962 A m^{-1}

[6] D. Raybould, K.S. Tan, J. Mater. Sci. 20 (1985) 2776–2786.
[7] W.J. Yuan, F.J. Liu, S.J. Pang, Y.J. Song, T. Zhang, Intermetallics 17 (2009) 278–280.
[8] A. Inoue, Acta Mater. 48 (2000) 279–306.
[9] T.P. Phway, A.J. Moses, J. Magn. Magn. Mater. 320 (2008) e611–e613.
[10] H. Ninomiya, Y. Tanaka, A. Hiura, Y. Takada, J. Appl. Phys. 69 (1991) 5358–5360.
[11] G.E. Fish, C.F. Chang, R. Bye, J. Appl. Phys. 64 (1988) 5370–5372.
[12] J. Guo, Y. Dong, Q. Man, Q. Li, C. Chang, X.M. Wang, R.W. Li, J. Magn. Magn. Mater. 401 (2016) 432–435.
[13] C. Chang, C. Qin, A. Makino, A. Inoue, J. Alloy. Compd. 533 (2012) 67–70.
[14] L. Xiaolong, D. Yaqiang, L. Min, C. Chuntao, W. Xin-Min, J. Alloy. Compd. 696 (2017) 1323–1328.
[15] A.H. Taghvaei, H. Shokrollahi, K. Janghorban, H. Abiri, Mater. Des. 30 (2009) 3989–3995.
[16] D. Jiles, IEEE Trans. Magn. 30 (1994) 4326–4328.

[17] A.H. Taghvaei, H. Shokrollahi, M. Ghaffari, K. Janghorban, J. Phys. Chem. Solids 71 (2010) 7–11.
[18] Y.B. Kim, D.H. Jang, H.K. Seok, K.Y. Kim, Mater. Sci. Eng. A 449-451 (2007) 389–393.
[19] H. Shokrollahi, K. Janghorban, J. Mater. Process. Technol. 189 (2007) 1–12.
[20] Y. Kang, Y. Huang, R. Yang, C. Zhang, J. Magn. Magn. Mater. 399 (2016) 149–154.
[21] Z. Wu, X.A. Fan, J. Wang, G. Li, Z. Gan, Z. Zhang, J. Alloy. Compd. 617 (2014) 21–28.
[22] J. Wang, X.A. Fan, Z. Wu, G. Li, J. Mater. Sci. 52 (2017) 7091–7099.
[23] X. Li, G. Lu, Z. Zhang, D. Ju, A. Makino, J. Alloy. Compd. 647 (2015) 917–920.
[24] Y.B. Kim, K. Kim, IEEE Trans. Magn. 42 (2006) 2802–2804.
[25] H.J. Liu, H.L. Su, W.B. Geng, Z.G. Sun, T.T. Song, X.C. Tong, Z.Q. Zou, Y.C. Wu, Y.W. Du, J. Supercond. Nov. Magn. 29 (2015) 463–468.
[26] T.H. Kim, K.K. Jee, Y.B. Kim, D.J. Byun, J.H. Han, J. Magn. Magn. Mater. 322 (2010) 2423–2427.
[27] Y.B. Kim, K.K. Jee, G.B. Choi, J. Appl. Phys. 103 (2008) 07E704.
[28] G.H. Kim, T.H. Noh, G.B. Choi, K.Y. Kim, J. Appl. Phys. 93 (2003) 7211–7213.
[29] H.Y. Choi, S.J. Ahn, T.H. Noh, Phys. Status Solidi A 201 (2004) 1879–1882.